

## Doorway states in $s$ -, $p$ -, and $d$ -wave entrance channels in $^{207}\text{Pb} + n$ reaction\*

D. J. Horen, J. A. Harvey, and N. W. Hill

Oak Ridge National Laboratory, Oak Ridge, Tennessee 37830

(Received 31 January 1978)

The  $^{207}\text{Pb} + n$  reaction has been studied by means of high resolution neutron transmission and differential elastic scattering measurement. Information pertaining to resonance parameters ( $E_n, l, J$ , and  $\Gamma_n$ ) for some 118 resonances in the energy interval from 3 to 485 keV has been obtained. Distributions of neutron strengths have been determined for each value of  $J$  that can be formed by  $s$ -,  $p$ -, and  $d$ -wave neutrons interacting with the  $^{207}\text{Pb}$  ground state ( $J^\pi = 1/2^-$ ). The existence of a doorway state in the  $J^\pi = 1^-$ ,  $s$ -wave channel at  $\sim 500$  keV is confirmed. Evidence is also found for the presence of doorway states in the  $p$ -wave ( $J^\pi = 1^+$ ) and  $d$ -wave ( $J^\pi = 1^-$ ) channels. The doorway state in the  $p$ -wave channel is shown to be correlated with  $M1$  ground-state radiative strength in  $^{208}\text{Pb}$ . In the energy region above the doorway state, the "average"  $p$ -wave strength function for forming  $1^+$  resonances [ $S^1(1^+) = (6.8 \pm 0.6) \times 10^{-5}$ ] is found to be equal to the sum of those for forming  $0^+$  [ $S^1(0^+) = (4.2 \pm 1.0) \times 10^{-5}$ ] and  $2^+$  [ $S^1(2^+) = (2.8 \pm 0.4) \times 10^{-5}$ ] resonances in agreement with predictions of the random phase assumption.

NUCLEAR REACTIONS  $^{207}\text{Pb}(n), (n, n)$ ,  $E = 3\text{--}485$  keV; measured  $\sigma_T(E)$ ,  $\sigma(E, \theta)$ .  $^{208}\text{Pb}$  deduced doorway states, resonance parameters,  $J^\pi$ ,  $\Gamma_n$ , neutron strength functions.

### INTRODUCTION

During the past fifteen years, there have been a number of theoretical efforts to describe the interaction of neutrons with nuclei in the region of discrete resonances. Much of this discussion has centered upon the description of fluctuations or fine structure in nuclear cross sections and their interpretation in terms of giant resonances and doorway states. One school of thought has evolved from the ideas put forth by Block and Feshbach<sup>1</sup> and extended by others.<sup>2</sup> Here one visualized the initial neutron scattering (on an even-even target) to involve the excitation of a  $2p\text{-}1h$  state as a possible doorway state. Successive scatterings would entail states of higher complexity. A second approach has been the more general theory of nuclear reactions discussed by Lane and Robson.<sup>3</sup>

From studies of neutron scattering by a series of lead isotopes, the group at Duke University observed a doorway state which was common to the  $^{206}, ^{207}, ^{208}\text{Pb} + n$  reactions.<sup>4</sup> This doorway state was reasonably well described in terms of a ( $2g_{9/2}, 4^+$ ) particle-core excitation by Beres and Divadeenam.<sup>5</sup>

In this work we report on high resolution neutron transmission and differential elastic scattering measurements on  $^{207}\text{Pb}$ . The results of earlier transmission measurements, much of which were done with considerably poorer energy resolution, have been summarized by Mughabghab and Garber.<sup>6</sup> The correlation of data pertaining to levels in the unbound region of  $^{208}\text{Pb}$  obtained from studies

of neutron scattering and capture on  $^{207}\text{Pb}$  and the  $^{208}\text{Pb}(\gamma, n)$  reaction have been hindered by a lack of high resolution measurements. This has resulted in considerable confusion as to level spin and parity assignments, as well as to such questions as the location of  $M1$  strength in  $^{208}\text{Pb}$ . Portions of our results have been reported elsewhere.<sup>7</sup>

### EXPERIMENTAL

High resolution neutron transmission and elastic scattering measurements were performed at the Oak Ridge Electron Linear Accelerator (ORELA) utilizing 80- and 200-m flight paths. Details of the experimental methods employed to obtain transmission data at ORELA can be found in Ref. 8, which discusses typical neutron sources, beam filters, detectors, data accumulation, and data reduction (including sources of background) procedures. Only those aspects which relate specifically to this experiment will be given here.

For neutron energies greater than about 15 keV, transmission data were taken at 200 meters using an electron beam of 5-ns duration at a repetition rate of  $800 \text{ sec}^{-1}$  striking a Be-clad, water-moderated, tantalum target. Filters of 3.0 cm of uranium and  $0.3 \text{ g/cm}^2$   $^{10}\text{B}$  were inserted prior to the lead sample in order to reduce the  $\gamma$  flash at the detector and to eliminate the overlap of low-energy neutrons from following bursts. The neutron detector was a 7.62-cm diameter by 2.0-cm thick NE-110 plastic scintillator mounted upon an RCA-4522 photomultiplier. To obtain

the neutron transmission for  $^{207}\text{Pb}$ , data were recorded by cycling two lead samples in and out of the beam. One sample was enriched to 92.4%  $^{207}\text{Pb}$  and the other consisted of appropriate thicknesses of natural and radiogenic lead (88.3%  $^{206}\text{Pb}$ ) chosen so as to compensate the  $^{206}, ^{208}\text{Pb}$  content in the  $^{207}\text{Pb}$  sample. For these measurements we used a sample thickness of  $n = 0.1503$  atoms/b. For the energy interval between 15 and 75 keV the transmission was measured with a thin uncompensated  $^{207}\text{Pb}$  sample which has  $n = 0.0184$  atoms/b. Below 15 keV we used the flux which penetrated a 0.635-cm thick natural lead sample as recorded with a Li-glass detector at an 80-m flight path. Here, we assumed that the off-resonance cross section was constant over the width of the resonance and formed the transmission spectrum near each resonance by dividing the number of counts at each channel by the number of counts in a channel adjacent to the resonance.

The neutron energy resolution was determined phenomenologically from an examination of narrow resonances and found to be reasonably represented by the expression

$$(\Delta E/E)^2 = a + bE_n,$$

where  $a$  and  $b$  are  $0.20 \times 10^{-6}$  and  $0.50 \times 10^{-6}$   $\text{MeV}^{-1}$ , respectively. The determined value of  $a$  is somewhat larger than the value of 0.09 calculated from the geometry of the effective thicknesses of the neutron source and detector, whereas  $b$  is about as expected for the neutron pulse width and flight path used.

The neutron scattering measurements were made at both 80- and 200-m flight paths with beam bursts of 5 and 8 ns. The lead target was a disk 7.0-cm diameter and 0.5-cm thick. The target was located in an air gap of about 130 cm between the exit of the flight tube and the entrance of an evacuated extension tube. The neutron beam was collimated to 7.6-cm diameter. Two or three neutron detectors similar to that used for the transmission measurements were located at 25.4 cm from the center of the lead scatterer. One detector was usually fixed at  $90^\circ$  to serve as a beam monitor, and the others were rotated to various angles. At each angle, the sample was removed to determine the background due to scattering by the air. Measurements made with a carbon scatterer (which has no resonances below 2 MeV) were used to determine the product of the energy distribution of the incident neutron flux and the efficiency of the detector.

#### DATA ANALYSIS

The transmission data were corrected for background ( $\approx 1\%$ ), converted to an energy scale, and

analyzed by means of three computer programs (DCON, SIOB, and MULTI) which fold in the Doppler broadening and the experimental energy resolution. DCON<sup>9</sup> is a single-neutron channel, single-level Breit-Wigner formula. This formalism partially accounts for level-level interference and is applicable in regions which do not contain overlapping resonances with the same  $J^\pi$ . It can be used to simulate a two-neutron channel situation if the potential phase shift for one channel and the radiation width can be ignored.

The program MULTI<sup>11</sup> calculates the total cross section (restricted to one neutron channel) by means of the  $R$ -matrix theory of nuclear reactions.<sup>12</sup> Here the total cross section is expressed as

$$\sigma_T = \sum_J \sigma_{nT}^J = 2\pi\lambda^2 \sum_J g(J) \text{Re}(1 - U_{nn}^J),$$

$$U_{nn}^J = e^{-2i\phi_i} \frac{1 - R_i^J(S_i - B_i^J - iP_i)}{1 - \bar{R}_i^J(S_i - B_i^J + iP_i)},$$

$$R_i^J = \sum_\lambda \frac{\gamma_{i\lambda} \gamma_{i\lambda}}{E_\lambda - E - i\Gamma_{\gamma\lambda}/2}.$$

In these expressions  $R_i^J$  is the  $R$  matrix, assuming that the only open channels are elastic neutron scattering and photon emission;  $\gamma_{i\lambda}$  and  $\Gamma_{\gamma\lambda}$  are the neutron reduced width amplitude and the radiation width, respectively, for the  $\lambda$ th resonance. The  $\phi_i$ ,  $S_i$ ,  $B_i$ , and  $P_i$  represent the usual hard sphere phase shifts, shift factors, energy independent boundary conditions, and penetration factors, respectively. In this work we set  $B_i^J = S_i$ .

Most of the analysis up to 395 keV was carried out with SIOB. In regions where the data were analyzed with both SIOB and MULTI, the resonance parameters obtained from each program agreed within the quoted uncertainties. For resonances which have neutron widths comparable to or greater than the experimental resolution, the spin and  $\Gamma_n$  can be reliably deduced from analysis of the transmission data. In addition, where the interference effects between resonance and potential scattering were sufficiently large it was also possible to determine the  $l$  wave involved, and hence the parity of the resonance. Usually, resonances formed by  $s$ -wave neutrons can easily be recognized by this means. The fact that some of the  $J^\pi = 1^-$  (i.e.,  $s$  wave) resonances observed here have fairly large  $d$ -wave admixtures has been reported previously.<sup>7</sup>

The  $^{207}\text{Pb}$  potential phase shifts for  $l \geq 1$  are fairly small for  $E_n \lesssim 200$  keV. Hence, it was not possible to determine from the transmission data the parity for resonances formed by neutrons which differ by only one unit of angular momen-

tum. However, application of the formulas derived by Blatt and Biedenharn<sup>13</sup> for differential elastic scattering from isolated resonances indicated that such a distinction could be made fairly easily. For the case under study here the shapes and/or relative magnitudes of the calculated resonance cross sections [i.e.,  $\sigma(E, \theta)$ ] are quite sensitive to the  $l$  value by which the resonance is formed. In particular,  $l=1$  resonances are distinguishable by their asymmetric shapes in the forward and backward hemispheres. In the forward hemisphere (e.g., at  $45^\circ$ ) the cross section  $\sigma(E, \theta)$  rises sharply below the resonance energy and falls off slowly above (see, e.g., the 115-keV resonance in Fig. 1). This asymmetry is reversed in the backward hemisphere (e.g., at  $135^\circ$ ). On the other hand, resonances with  $l=2$  have symmetric shapes in the forward and backward hemispheres (e.g., see the 209-keV resonance in Fig. 2). The  $l=1$  resonances appear symmetric at  $90^\circ$  while the  $l=2$  resonances show interference effects. These characteristic features have been used to assign  $l$  values to most of the resonances for which  $\Gamma_n$  was found to be comparable to or greater than the experimental energy resolution.

Additional assignments were possible for some of the narrow resonances where the data were sufficient to determine the relative cross sections as a function of angle. The  $l=1$  resonances are expected to have reduced cross sections at large angles due to the dominance of the  $P_1(\cos\theta)$  term, whereas the  $l=2$  resonances should have almost equal cross sections at  $45^\circ$  and  $135^\circ$ .

Since the main interest of the scattering measurements was to determine  $l$  values, emphasis was placed upon achieving high resolution and only relative cross sections, rather than accurate absolute ones. For most resonances a visual comparison of the scattering data with single-level calculations using the Blatt and Biedenharn<sup>13</sup> formula proved sufficient to specify  $l$  values. The potential phase shifts (mainly  $\phi_0$ ,  $\phi_1$ , and  $\phi_2$ ) used in the calculations were derived from the analysis of the transmission data or calculated using the hard-sphere expressions with effective radii given below.

Some typical elastic scattering spectra are shown in Figs. 1-4. Included also are some calculated spectra (i.e., resonance plus interference only) which were used as a guide for specifying  $l$  values. The calculated differential cross sections were normalized to the experimental data at  $45^\circ$ . Since  $^{207}\text{Pb}$  has a ground-state spin  $J=\frac{1}{2}$ , the channel spin can assume two values, i.e.,  $s=0$  or  $1$ . For those resonances (e.g.,  $J=1^+$ ) which could be formed via reactions involving both channel spins, the corresponding neutron widths were taken to

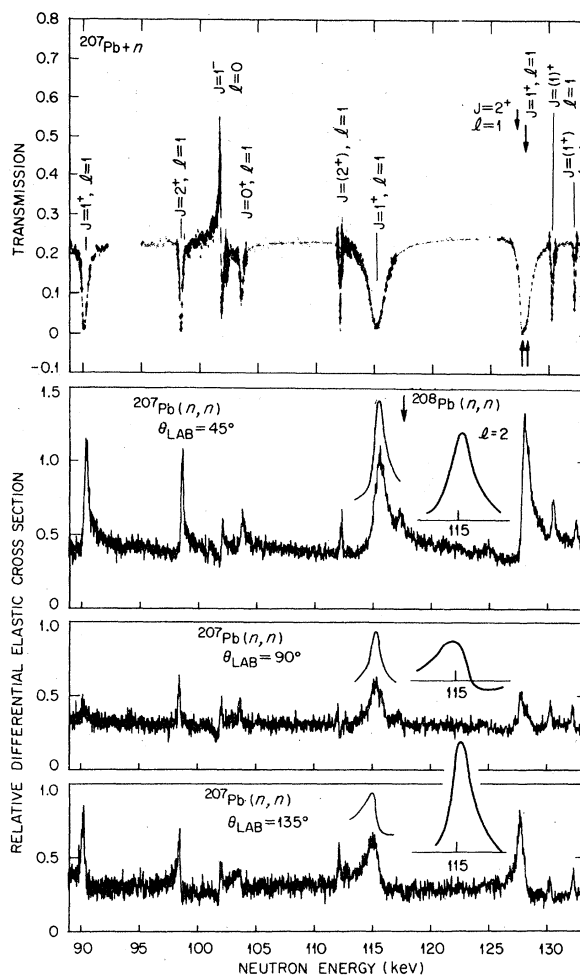


FIG. 1. Neutron transmission and differential elastic scattering spectra for  $^{207}\text{Pb}$  in the energy interval 85–135 keV. The differential cross sections are given in relative units. For comparison, calculated cross sections are shown for the 115.17-keV (resonance plus interference only) resonance (assuming  $l=0$  or  $2$ ) normalized to the same relative scale as the experimental data at  $45^\circ$ . The potential phase shifts were taken as  $\phi_0 = -40.1^\circ$  and  $\phi_1 = 1.3^\circ$ . Phase shifts for the higher  $l$  waves were set equal to zero.

be equal in the calculations.

Transmission spectra for the energy interval  $E_n = 65$  to 485 keV are shown in Figs. 5–7. The lines through the data points represent the results of least square fits obtained with SIJOB. In this program, the shift factor and penetrability (i.e.,  $S_l$  and  $P_l$ ) are assumed to be functions of  $ka$ , where  $a$  is the “channel radius” taken as  $a = 8.042$  fm in this work, whereas the potential shifts are functions of  $kR$ . Here,  $R$  represents an “effective radius” and is a variable in the search procedure along with the resonance pa-

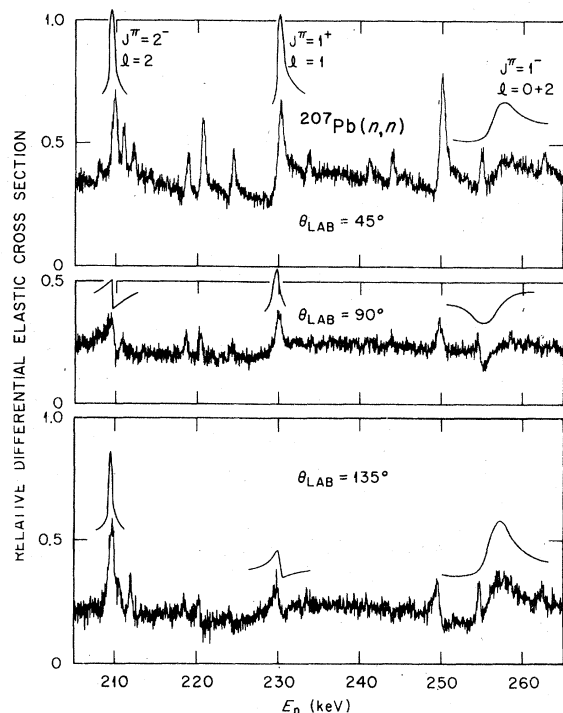


FIG. 2. Relative differential elastic scattering spectra for  $^{207}\text{Pb}$  in the energy interval 205–265 keV. Calculated spectra are shown for resonances at 209.45 ( $l = 2$ ,  $J^\pi = 2^-$ ), 229.77 ( $l = 1$ ,  $J^\pi = 1^+$ ), and 256.43 ( $l = 0 + 2$ ,  $J^\pi = 1^-$ ). Potential phase shifts used in the calculations were deduced from analyses of the transmission data.

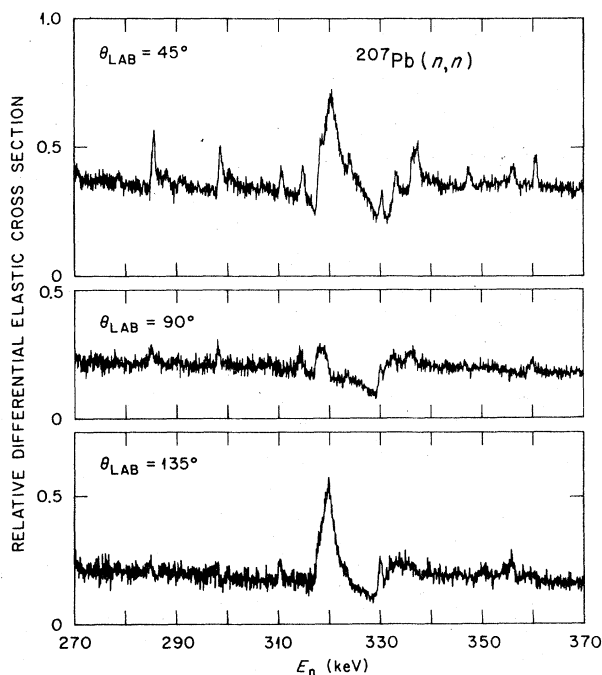


FIG. 3. Relative differential elastic scattering spectra for  $^{207}\text{Pb}$  in the energy interval 270–370 keV.

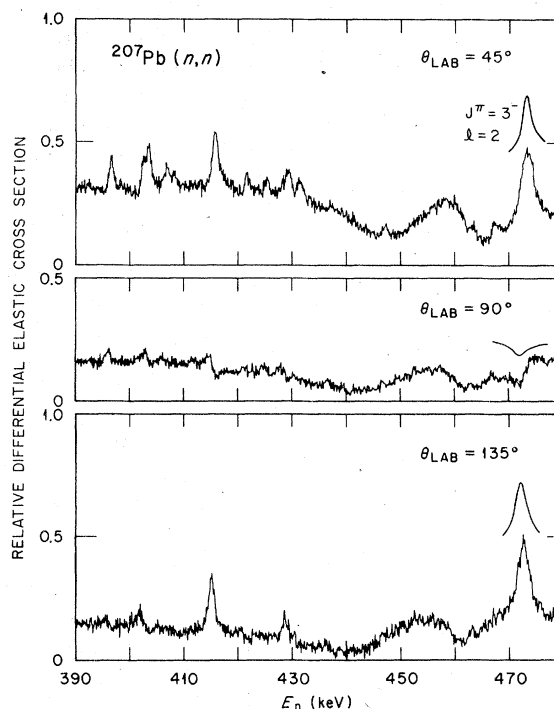


FIG. 4. Relative differential elastic scattering spectra for  $^{207}\text{Pb}$  in the energy interval 390–480 keV. Calculated spectra for the resonance at 472.5 ( $l = 2$ ,  $J^\pi = 3^-$ ) keV are shown for comparison.

rameters. It was found that the value of  $R$  needed to fit the  $p$ -wave resonances differed from that required by  $s$  waves. The data between 60–390 keV were well fitted with  $R_s = R_d = 9.3 \pm 0.5$  fm and  $R_p = 6.3 \pm 0.3$  fm.

The data for the energy interval 390–500 keV are shown in Fig. 8, where the cross section rather than transmission is plotted. These data were analyzed with MULTI where the channel radius was also taken as 8.042 fm. As might be expected, the data show considerable interference between the two  $s$ -wave resonances with  $J^\pi = 1^-$  at 447.2 ( $\Gamma_n = 18.8$  keV) and 463.9 ( $\Gamma_n = 11.9$  keV) keV. The lack of a better fit in this region ( $\approx 456$  keV) might indicate a  $d$ -wave admixture in one or both of these resonances. We see no evidence for  $s$ -wave resonances with  $J^\pi = 0^-$  which were reported by Seibel *et al.*<sup>4</sup> at 460 ( $\Gamma_n = 45$  keV) and 480 ( $\Gamma_n = 10$  keV) keV. The latter work was performed with considerably poorer resolution than achieved here.

A summary of the resonances analyzed in this work is given in Table I. The value of  $\Gamma_n$  obtained by analysis using the computer code SIOB is essentially the same as would result by calculating the resonance shape with a single-level formula. As noted above, the code MULTI deduces the value

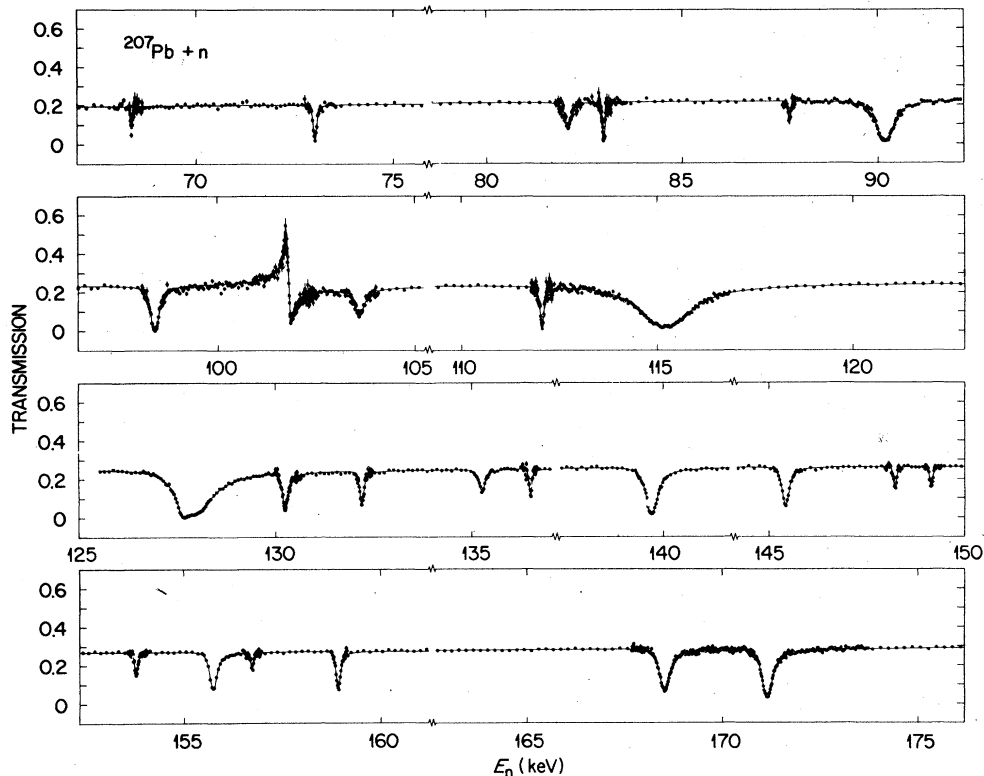


FIG. 5. Neutron transmission for  $^{207}\text{Pb}$  in the energy interval 65–175 keV. The solid curve through the points represents a single-channel, multilevel fit to the data.

of  $\gamma^2$  rather than  $\Gamma_n$ . Where MULTI was used  $\Gamma_n$  was calculated as  $\Gamma_n = 2P_1\gamma^2$ . For our particular problem, this expression also gives a value of  $\Gamma_n$  as would be obtained from a single-level analysis except for those resonances whose shapes are altered considerably because of interference effects arising from nearby resonances. For those resonances which were analyzed by means of both SIOB and MULTI, the corresponding values of  $\Gamma_n$  agreed with each other within the quoted experimental uncertainties. Since most previously reported transmission measurements have been performed with much poorer energy resolution, it does not seem warranted to make a detailed comparison here with those results. Suffice it to say that in general we have observed many more resonances, and, except for the very broad ones, we invariably find much smaller  $\Gamma_n$  values than those which have been reported earlier.<sup>6, 14</sup>

The resonances at 181.49, 256.43, and 316.97 keV have figured prominently in searches for  $M1$  radiation in  $^{208}\text{Pb}$ . Our results clearly show that these resonances have  $J^\pi = 1^+$ , and we have already<sup>7</sup> discussed their  $(s+d)$ -wave admixtures. Recently, Holt *et al.*<sup>15</sup> obtained photoneutron po-

larization data for the 181.49- and 256.43-keV resonances in agreement with  $1^+$  assignments. The occurrence of close lying  $J^\pi = 1^+$  resonances as well as the possibility of  $(s+d)$ -wave admixtures show that care must be exercised in the analysis of neutron capture or photoneuclear data pertaining to those two resonances. Bowman *et al.*<sup>16</sup> and Toohey and Jackson<sup>17</sup> have reported the photoneuclear angular distribution for the 256.43-keV resonance to be isotropic. However, in both cases the experimental resolution was such as to include contributions (if present) from the  $1^+$  resonance at 249.88 keV. In later photoneuclear works,<sup>18</sup> an isotropic distribution for the 256.43-keV resonance has been used as the basis for normalizing angular distribution data for other measured resonances.

In addition to the resonances listed in Table I, the transmission data contained a number of others for which the neutron width was very much smaller than the experimental energy resolution. Although no attempt was made to analyze these, their energies are tabulated in Table II. Some of these resonances have been reported in studies of the  $^{207}\text{Pb}(n, \gamma)$  and  $^{208}\text{Pb}(\gamma, n)$  reactions.

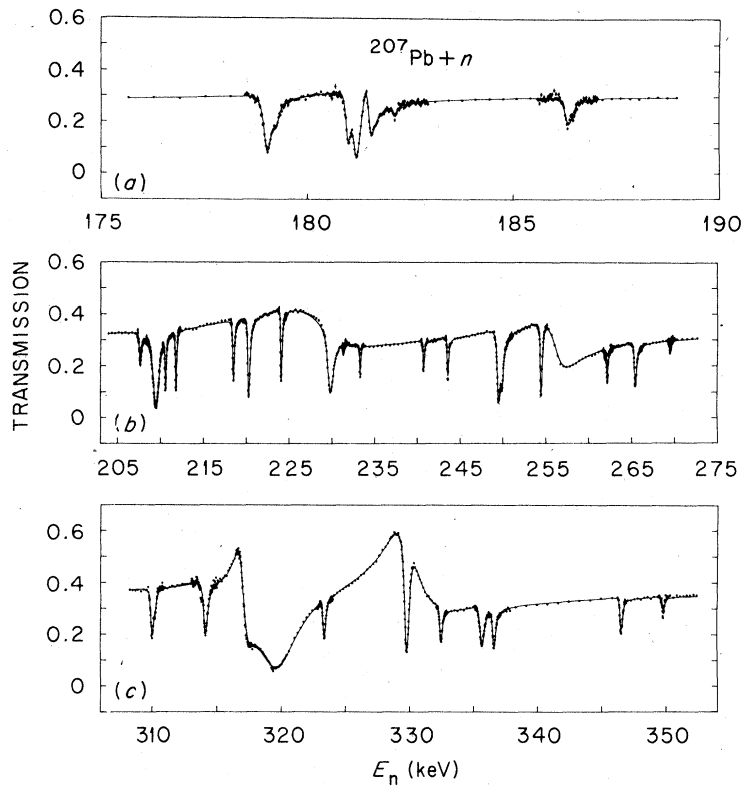


FIG. 6. Neutron transmission for  $^{207}\text{Pb}$  in the energy interval 175–350 keV. The solid curve through the points represents a single-channel, multilevel fit to the data. The two resonances at 181.49 and 256.43 keV ( $l = 0 + 2$ ,  $J^\pi = 1^-$ ) have each been fitted by use of two resonances at the same energy, one with  $l = 0$  and the other with  $l = 2$ . The  $d$ -wave potential phase shifts were assumed to be zero. This approximation was adequate because  $\phi_2 \approx -1.0^\circ$ , and is equivalent to a two-channel, single-level formula with  $s + d$  admixture.

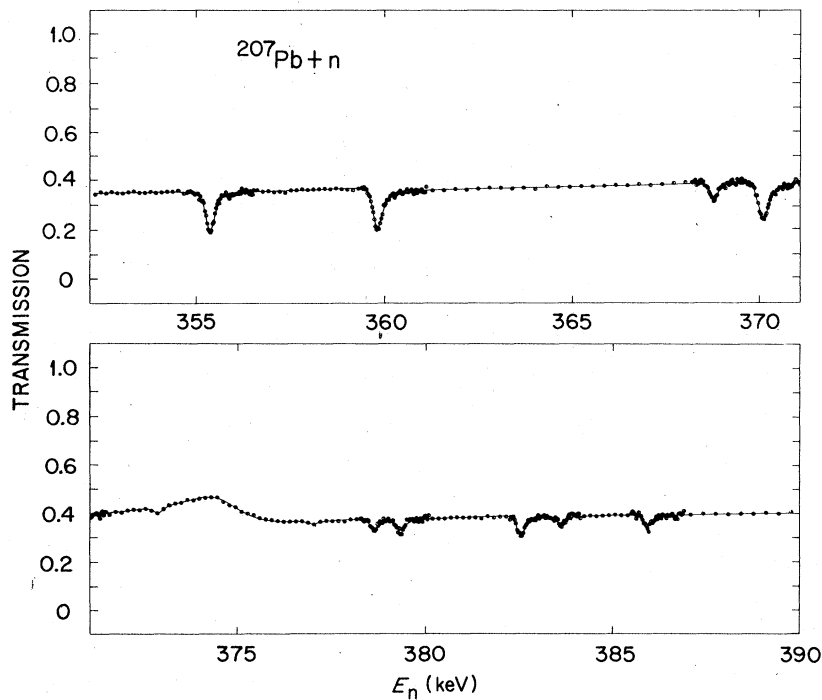


FIG. 7. Neutron transmission for  $^{207}\text{Pb}$  in the energy interval 350–385 keV. (See caption to Fig. 5.)

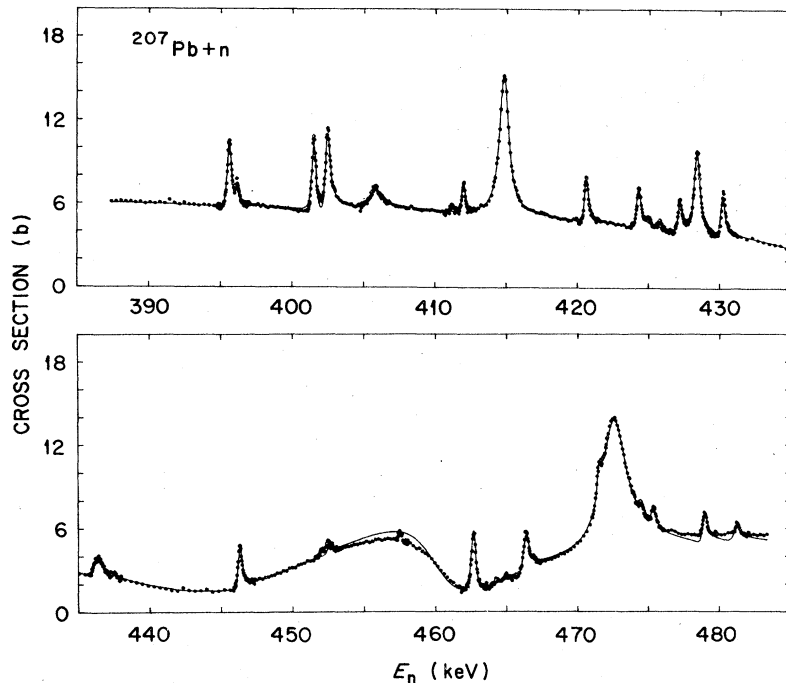


FIG. 8. Neutron total cross section of  $^{207}\text{Pb}$  in the energy interval 385–485 keV. The solid line through the points represents a single-channel, multilevel fit to the data.

## DISCUSSION

### $l = 0$ resonances

Up to an energy of  $E_n = 490$  keV we observe only two  $J^\pi = 0^-$  and eight  $J^\pi = 1^-$   $s$ -wave resonances. The sum of the reduced neutron widths ( $\Gamma_n^0$ ) is plotted versus neutron energy for each  $J$  value in Fig. 9. Here  $\Gamma_n^l$  is the reduced neutron width defined as

$$\Gamma_n^l = \frac{\Gamma_n}{v_l} \frac{(1 \text{ eV})^{1/2}}{(E_n)^{1/2}},$$

where the neutron width  $\Gamma_n$  and  $E_n$  are given in electron volts and  $v_l$  is the penetrability factor for a neutron having angular momentum  $l$ . (Throughout this work we have calculated penetrability factors using a radius of 8.042 fm.) Our results for the  $1^-$  resonances are similar to those previously reported by Seibel *et al.*<sup>4</sup> although the latter did not observe the resonances at 101.80, 181.49, 256.43, and 316.97 keV. Seibel *et al.*<sup>4</sup> pointed out that the change in  $s$ -wave strength function near 450 keV (i.e., change in slope of  $\sum \Gamma_n^0$  versus  $E_n$ ) for the  $1^-$  resonances might be interpreted in terms of a "doorway state" which is common to the  $^{206, 208}\text{Pb} + n$  reactions. These authors reported additional  $1^-$ ,  $s$ -wave resonances above 490 keV. Although these are also present in our data, they have not as yet been analyzed here. Seibel *et al.*<sup>4</sup> showed that

with the addition of the  $1^-$  resonances above 490 keV the strength function above the doorway state (i.e.,  $\approx 450$  keV) tends toward its value below. It is clear from Fig. 9 that the  $s$ -wave strength function below the region of the doorway state is quite small (i.e.,  $S^0 < 5 \times 10^{-5}$ ). This is a reflection of the fact that the  $4s$  single-particle state is bound by 2 MeV in  $^{208}\text{Pb}$ .

Seibel *et al.*<sup>4</sup> also reported a doorway state in the  $0^-$  channel at about 460–480 keV. However, as noted earlier, we do not observe a  $J^\pi = 0^-$  resonance in that energy region. In fact there is no indication of another  $0^-$  resonance in our data between the 374.75-keV resonance and 590 keV.

Divadeenam *et al.*<sup>5</sup> showed that  $s$ -wave doorway states at  $E_n \approx 500$  keV in the  $^{206, 207, 208}\text{Pb} + n$  compound systems could be described qualitatively in terms of a common particle-vibration interaction involving the  $^{208}\text{Pb}$  core (i.e.,  $4^+ \otimes \nu g_{9/2}$ ). This model also predicted a single doorway state in the  $0^-$  channel with an escape width comparable to that in the  $1^-$  channel, and located at about the same energy of excitation. On the other hand, results of  $1p-1h$  calculations (see e.g., Ref. 19) indicate that more than one  $0^-$  (and two  $1^-$ ) state ( $s$ ) may be present in this energy region. Hence, it is conceivable that the strength of the  $0^-$  doorway state may not be localized. In this regard, we note that the reduced width of the  $0^-$  resonance at 228.49 keV is comparable to those of

TABLE I. Resonance parameters for  $^{207}\text{Pb}+n$ .

$E_n$ (keV)	$l$	$J^\pi$	$\Gamma_n$ (eV)	$\Gamma_n^{\text{a}}$ (eV)	
3.063	8	(1) <sup>b</sup>	0.12	5	0.23
10.185	8	(1) <sup>b</sup>	~0.9 <sup>c</sup>		
12.357	8	(1) <sup>b</sup>	~1.1 <sup>c</sup>		
16.758	8	1 <sup>d</sup>	37	4	5.8
29.39	2	1 <sup>d</sup>	16	3	1.12
37.72	2	1 <sup>d</sup>	50	10	2.47
41.268	10	0	1 220	30	6.01
68.36	1	(1) <sup>b</sup>	7 <sup>c</sup>	5	
73.01	1	1 <sup>d</sup>	40	7	0.78
82.07	1	1	117	15	2.04
82.98	1	1 <sup>d</sup>	29 <sup>c</sup>	5	
87.74	1	(1) <sup>b</sup>	10 <sup>c</sup>	4	
90.17	2	1 <sup>d</sup>	272	13	4.14
98.39	2	1 <sup>d</sup>	103	10	1.42
101.80	2	0 <sup>g</sup>	70	4	0.23
103.57	3	1 <sup>d</sup>	250	20	3.19
112.05	3	(1)	45	8	0.52
115.17	2	1 <sup>d</sup>	923	30	10.36
127.66	5	1 <sup>d</sup>	140	30	1.37
127.91	5	1 <sup>d</sup>	613	60	6.06
130.23	2	1 <sup>d</sup>	87	9	0.84
132.18	4	(1)	55	7	0.52
135.25	4	1	133	10	1.23
136.49	4	(1)	18	4	0.16
139.69	4	1 <sup>d</sup>	168	10	1.49
145.41	4	1 <sup>d</sup>	115	8	0.96
148.22	4	(1)	~23		~0.18
149.14	4	(1)	~22		~0.17
153.77	4	(1)	~25		~0.20
155.73	4	1 <sup>d</sup>	115	8	0.87
156.72	5	(1)	11 <sup>c</sup>	4	
158.90	8	1 <sup>d</sup>	56 <sup>c</sup>	9	
168.51	5	1 <sup>d</sup>	192	8	1.36
171.13	5	1 <sup>d</sup>	160	6	1.13
179.01	8	1 <sup>d</sup>	134	20	0.86
179.23	10	1 <sup>d</sup>	59	10	0.44
180.98	8	1 <sup>d</sup>	73	15	0.45
181.18	5	1 <sup>d</sup>	87	10	0.56
181.49	10	0+2	60+32		0.14+2.80
182.10	10	(1)	26	10	0.18
186.32 <sup>f</sup>	8	(1)	156	20	1.04
199.52	8	(1)	62	20	0.36
200.99	10	(1)	~8 <sup>c</sup>		
207.62	8	1 <sup>d</sup>	236	20	1.33
209.45	8	2 <sup>d</sup>	490	30	29.0
210.55	10	1 <sup>d</sup>	66	9	0.37
211.77	10	2 <sup>d</sup>	70	15	4.10
218.45	8	1 <sup>d</sup>	132	20	0.70
220.23	8	1 <sup>d</sup>	163	23	0.85
224.00	8	1 <sup>d</sup>	83	17	0.42
228.49	10	0	10 380	200	21.7
229.77	8	1 <sup>d</sup>	586	20	2.93
233.26	10	(1) <sup>g</sup>	53	12	0.26
240.67	10	1 <sup>d</sup>	58	18	0.28
243.51	10	1 <sup>d</sup>	92	25	0.43
249.49	8	1 <sup>d</sup>	300	30	1.38
249.88	10	1 <sup>d</sup>	138	40	0.69
254.44	8	2 <sup>d</sup>	111	20	4.22
256.43	25	0+2	1 720+1 390		3.40+52.5

TABLE I. (Continued)

$E_n$ (keV)	$l$	$J^\pi$	$\Gamma_n$ (eV)	$\Gamma_n^{\text{a}}$ (eV)
262.16	15	1 <sup>d</sup>	(1) <sup>+</sup>	89 22 0.39
265.44	8	1 <sup>d</sup>	1 <sup>+</sup>	182 20 0.78
269.45	20	(1)	(0 <sup>+</sup> )	52 20 0.22
276.44	20	(1)	(0 <sup>+</sup> )	76 25 0.32
284.68	10	1 <sup>d</sup>	(1) <sup>+</sup>	87 20 0.35
285.02	8	1 <sup>d</sup>	(2) <sup>+</sup>	115 16 0.46
287.44	10	(1)	(1 <sup>+</sup> )	66 15 0.26
290.19	10	1	0 <sup>+</sup>	160 20 0.63
296.47	10	(1)	(0 <sup>+</sup> )	44 15 0.17
297.97	8	1 <sup>d</sup>	1 <sup>+</sup>	314 28 1.20
299.89	10	(1)	(1 <sup>+</sup> )	48 15 0.18
301.39	10	(1)	(0 <sup>+</sup> )	73 20 0.28
306.11	10	(1)	(1 <sup>+</sup> )	36 10 0.13
309.97	10	2 <sup>d</sup>	(2) <sup>-</sup>	86 15 2.15
310.21	8	(2)	(1 <sup>-</sup> )	43 15 1.1
314.08	10	1 <sup>d</sup>	1 <sup>+</sup>	217 15 0.76
316.97	10	0+ (2)	1 <sup>-</sup>	850+ (~100) 1.51+ (~2.4)
317.4	2	(1)	(0 <sup>+</sup> )	~900 ~3.2
319.56	10	2 <sup>d</sup>	2 <sup>-</sup>	2680 150 62.1
323.32	10	1 <sup>d</sup>	2 <sup>+</sup>	79 10 0.27
329.74	10	2 <sup>d</sup>	3 <sup>-</sup>	234 20 5.25
330.24	30	0+ (2)	1 <sup>-</sup>	3080+ (~470) 5.36+ (~10.4)
332.41	8	1 <sup>d</sup>	(2) <sup>+</sup>	78 10 0.27
335.61	8	1 <sup>d</sup>	1 <sup>+</sup>	254 20 0.85
336.55	8	1 <sup>d</sup>	(2) <sup>+</sup>	115 20 0.38
346.48	8	(1) <sup>d</sup>	(2 <sup>-</sup> )	70 20 0.23
349.76	10	(1, 2)	(2 <sup>+</sup> )	35 <sup>c</sup> 9
355.36	10	2 <sup>d</sup>	2 <sup>-</sup>	105 15 1.99
359.78	10	1 <sup>d</sup>	2 <sup>+</sup>	105 20 0.33
368.77	10	(1) <sup>b</sup>	(1 <sup>+</sup> ) <sup>b</sup>	52 10 0.16
370.08	10	1 <sup>d</sup>	1 <sup>+</sup>	172 22 0.53
372.86	10	(1)	(0 <sup>+</sup> )	~33 ~0.1
374.75	10	0	0 <sup>-</sup>	1970 90 3.21
376.97	10	(1)	(0 <sup>+</sup> )	~35 ~0.11
378.60	10	(1)	(0 <sup>+</sup> )	98 30 0.29
379.29	10	(1)	(1 <sup>+</sup> )	43 15 0.13
382.52	10	(1)	(1 <sup>+</sup> )	64 15 0.19
383.58	10	(1)	(0 <sup>+</sup> )	66 20 0.20
385.91	20	(1)	(1 <sup>+</sup> )	43 15 0.13
395.6 <sup>h</sup>		1 <sup>d</sup>	2 <sup>+</sup>	195 40 0.55
396.1		1 <sup>d</sup>	(0) <sup>+</sup>	142 30 0.41
401.6		1 <sup>d</sup>	2 <sup>+</sup>	215 35 0.61
402.4		1 <sup>d</sup>	2 <sup>+</sup>	239 40 0.68
405.7		1 <sup>d</sup>	0 <sup>+</sup>	839 80 2.37
412.0		1 <sup>d</sup>	(2) <sup>+</sup>	61 25 0.16
414.9		2 <sup>d</sup>	3 <sup>-</sup>	693 75 9.47
420.6		1 <sup>d</sup>	2 <sup>+</sup>	117 30 0.32
424.2		1 <sup>d</sup>	1 <sup>+</sup>	196 35 0.53
427.1		1 <sup>d</sup>	1 <sup>+</sup>	138 34 0.37
428.4		2 <sup>d</sup>	2 <sup>-</sup>	315 40 4.05
430.1		1 <sup>d</sup>	(2) <sup>+</sup>	97 30 0.26
436.3		1 <sup>d</sup>	0 <sup>+</sup>	667 75 1.76
446.3		1 <sup>d</sup>	2 <sup>+</sup>	116 30 0.30
447.2		0 <sup>e</sup>	1 <sup>-</sup>	~18800 ~28.1
462.7		2 <sup>d</sup>	3 <sup>-</sup>	162 40 1.79
463.9		0 <sup>e</sup>	1 <sup>-</sup>	~11900 ~17.5
466.3		1 <sup>d</sup>	(1) <sup>+</sup>	234 40 0.58
471.5		2 <sup>d</sup>	(2) <sup>-</sup>	~99 ~1.05
472.5		2 <sup>d</sup>	3 <sup>-</sup>	2079 300 22.0

TABLE I. (Continued)

<sup>a</sup>Reduced neutron width at 1 eV, calculated using a radius of 8.042 fm. Strictly speaking, the  $\Gamma_n^l$  derived from fits using **SI0B** should be multiplied by  $[1 + (R_i^{(0)}P_l)^2]^2$  to put them on the same basis as those from **MULTI**. However, in this work  $R_i^{(0)}P_l \ll 1$ , and this correction has been ignored.

<sup>b</sup>Assumed value. From transmission measurements  $l \neq 0$ .

<sup>c</sup>Values given are  $g\Gamma_n^l$ .

<sup>d</sup> $l$  determined from elastic scattering measurements.

<sup>e</sup>Possibly contains  $l=2$  admixture.

<sup>f</sup>Possible multiplet.

<sup>g</sup>Possibly  $l=2$ .

<sup>h</sup>Above 386 keV energy uncertainty  $\sim 0.2$  keV.

the  $1^-$  resonances at 447.2 and 463.9 keV. This might be an indication that the 228.49-keV resonance itself may form a part of a doorway state in the  $0^-$  channel.

From a plot of the number of  $l=0, J^\pi=1^-$  resonances versus  $E_n$ , we determine the average level spacing in the region 40–500 keV as  $\langle D \rangle_{1^-} = 58 \pm 15$  keV.

#### $l=1$ resonances

In Table I we have tabulated 93  $p$ -wave resonances. Of these, 22 are assigned as  $0^+$  (8 definite), 39, as  $1^+$  (with about 28 definite), and 26 as  $2^+$  (about 16 definite). Plots of  $\sum \Gamma_n^1$  vs  $E_n$  for each  $J$  value are shown in Fig. 10. In each case most of the strength is contained in resonances for which the  $J$  values are well determined. The change in the strength function near 120 keV for the  $1^+$  resonances has been interpreted<sup>7</sup> as a doorway state associated with the  $M1$  resonance in  $^{203}\text{Pb}$  which arises from the  $\pi h_{9/2} - \pi h_{11/2}^{-1}$  and  $\nu i_{11/2} - \nu i_{13/2}^{-1}$  particle-hole con-

figurations. From the slope in the energy region above this doorway state, i.e., 170–340 keV, we find the  $p$ -wave strength function for forming  $1^+$  levels as  $S^1(1^+) = (6.8 \pm 0.6) \times 10^{-5}$ . The reduction in slope above 340 keV could be the result of missed resonances. For the  $0^+$  resonances we find  $S^1(0^+) = (4.2 \pm 1.0) \times 10^{-5}$ . Here the uncertainty reflects the possibility that many of the resonances tentatively assigned as  $0^+$  might have other values of  $J$ . The strength function for forming  $2^+$  resonances is determined as  $S^1(2^+) = (2.8 \pm 0.4) \times 10^{-5}$ . The uncertainties for the strength functions quoted here do not account for possible effects due to missed resonances, which we estimate would be small.

If the compound nucleus theory and random phase assumptions are applicable (i.e., outside the region containing structure), the spin-spin interaction is negligible and the strength function depends only upon the orbital and total angular momenta (i.e.,  $l$  and  $j$ ), then the strength functions expressed in channel spin formalism are related<sup>20</sup> to those in spin-orbit formalism by means of Racah coefficients, i.e.,

$$S_s^i(J) = \sum_{j=|l-1/2|}^{l+1/2} (2j+1)(2s+1) W^2(ijJl; sj) \times S_j^i.$$

Here,  $s$  is the channel spin,  $i$  is the intrinsic spin of the neutron, and  $l$  is the spin of the target. For the case of  $^{207}\text{Pb} + n$  this relation leads to

$$\begin{aligned} S_1^1(0) &= S_{1/2}^1, \\ S_1^1(2) &= S_{3/2}^1, \\ S_0^1(1) &= \frac{1}{3} S_{1/2}^1 + \frac{2}{3} S_{3/2}^1, \end{aligned}$$

and

$$S_1^1(1) = \frac{2}{3} S_{1/2}^1 + \frac{1}{3} S_{3/2}^1.$$

From these relations it follows that the strength function  $S^1(1)$  for forming  $1^+$  states should just equal the sum of the strength functions for forming the  $0^+$  and  $2^+$  levels. Experimentally we find this to be in excellent agreement with our values quoted above. We determine the total  $p$ -wave strength function defined as the slope of the curve of  $(2l+1)^{-1} \sum_j g(J) \Gamma_n^1(J)$  versus  $E_n$  as  $S^1 = (3.5 \pm 0.6)$

TABLE II. Weak resonances observed in  $\sigma_T$  of  $^{207}\text{Pb} + n$  not analyzed in this work.

$E_n$ (keV) <sup>a</sup>	$E_n$ (keV) <sup>a</sup>
197.02	424.98
201.10	425.74
213.87	432.44
231.31	437.63
243.94	442.39
260.58	443.02
273.46	445.40
278.0	452.05
304.42	452.52
313.82	457.48
340.39	464.40
372.84	464.98
377.03	466.9
383.60	474.3
391.56	475.3
411.20	478.9
419.93	481.2

<sup>a</sup>Uncertainties in energy are about 0.03%.

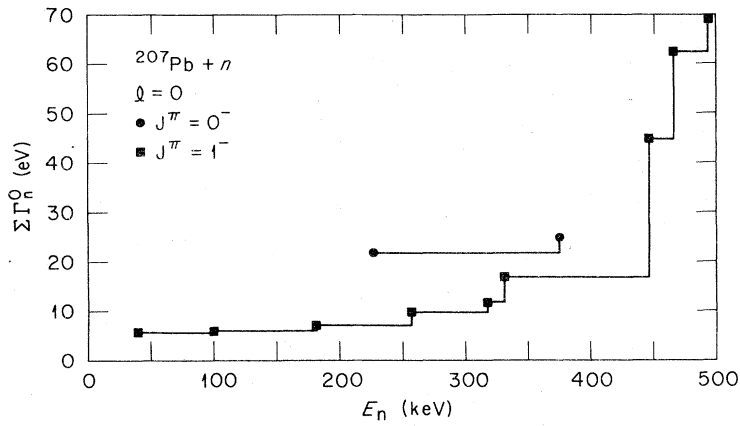


FIG. 9. Plots of the sum of reduced neutron widths ( $\sigma \Gamma_n^0$ ) for resonances formed by s waves versus neutron energy. The reduced widths were calculated using a nuclear radius of 8.942 fm.

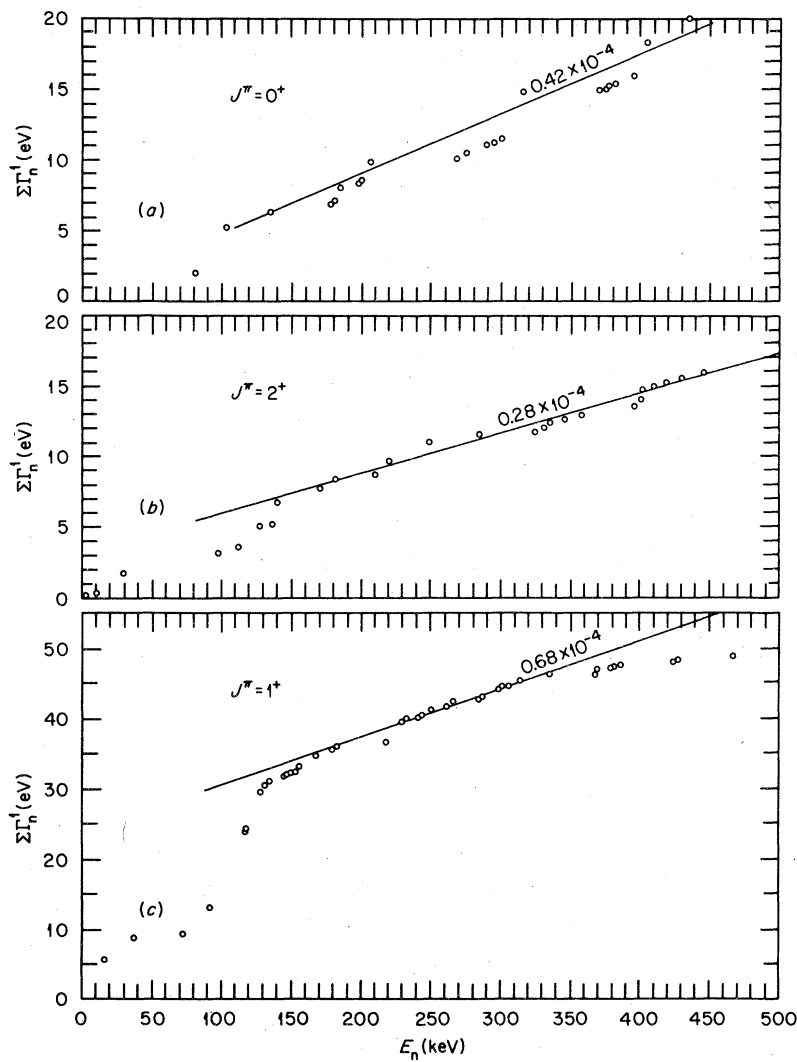


FIG. 10. Plots of the sum of reduced neutron widths ( $\sigma \Gamma_n^1$ ) for resonances formed by p waves versus neutron energy. (See caption to Fig. 9.)

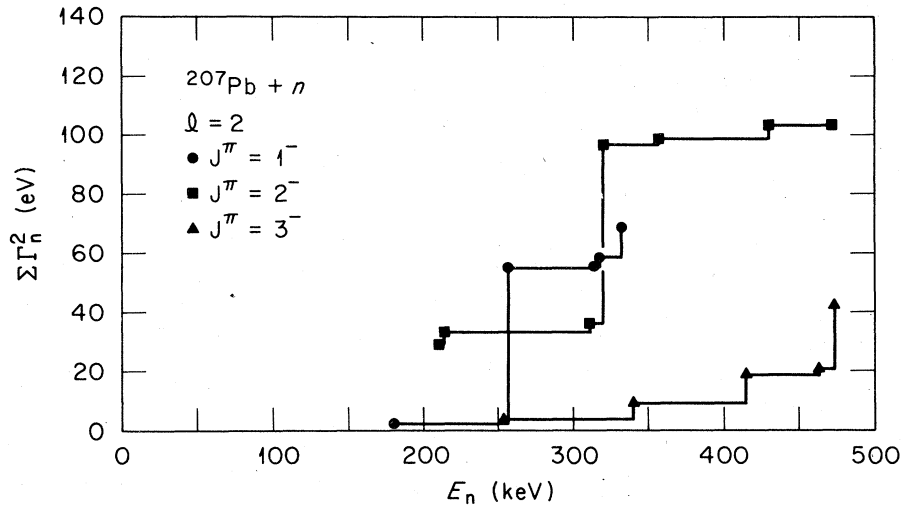


FIG. 11. Plots of the sum of reduced widths ( $\sigma \Gamma_n^2$ ) for resonances formed by  $d$  waves versus neutron energy. (See caption to Fig. 9.)

$\times 10^{-5}$ . Of course this is only valid for the energy interval  $150 \lesssim E_n \lesssim 350$  keV.

From a plot of the number of  $p$ -wave resonances (for all  $J$ ) versus  $E_n$  in the energy region 60–450 keV one can determine the average spacing of  $l=1$  resonances as  $\langle D_l \rangle \approx 4.3$  keV. We do not calculate here the average level spacing for each  $J$  value, as these are quite dependent upon the correctness of the tentatively assigned  $J$ 's as well as to possible missed resonances.

As can be seen in Fig. 10, the strength function for forming  $2^+$  resonances also seems to show structure in the vicinity of 100–150 keV, and this might be indicative of a doorway state in this

channel also. It is conceivable that such an effect might result from the recoupling of some of the configurations which give rise to the doorway state in the  $1^+$  channels. This point requires further study.

$l = 2$  resonances

Plots of  $\Sigma \Gamma_n^2$  vs  $E_n$  are shown in Fig. 11 for the resonances formed by  $d$ -wave neutrons. With such small statistical samples for each  $J$  value, it is difficult to determine whether it is significant that for each case one resonance accounts for most of the strength. However, since the width of the 256.43-keV resonance represents

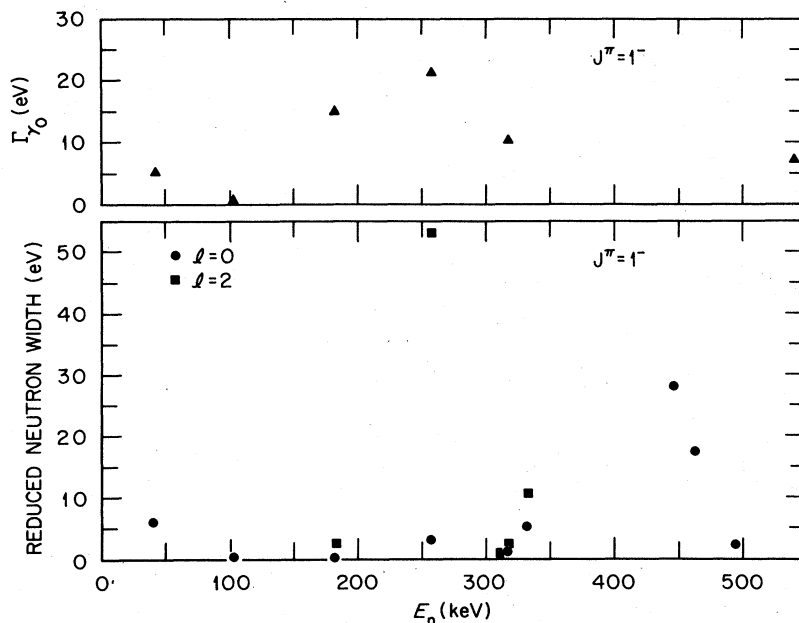


FIG. 12. Plots of reduced neutron widths and ground-state radiation widths versus neutron energy for  $J^\pi = 1^-$  resonances. The photon radiation widths are from Ref. 21.

an appreciable fraction of the Wigner limit, we decided to investigate the possibility that it might be associated with a doorway state in the  $J^\pi = 1^-$  channel. To do so, we plot in Fig. 12 the reduced neutron widths (for both  $l=0$  and 2) and  $\Gamma_{\gamma_0}$ <sup>21</sup> for  $1^-$  resonances as a function of  $E_n$ . The increase in  $\Gamma_{\gamma_0}$  strength in the vicinity of 256 keV suggests a correlation in the photon and  $d$ -wave neutron channels. Such a correlation might be expected if a fragment of the  $\nu(3d_{3/2}, 3p_{1/2}^{-1})$  were localized near this energy of excitation since such a configuration could lead to a good overlap between the initial and final states in both the  $E1$  photon (i.e.,  $\Gamma_{\gamma_0}$ ) and  $d$ -wave neutron channels.

Ignoring the possible effects of microstructure, we have determined the total  $d$ -wave strength function between 180–480 keV as  $S^2 \approx 2.8 \times 10^{-4}$ .

### CONCLUSIONS

The  $^{207}\text{Pb} + n$  reaction has been investigated by means of high resolution neutron transmission and differential elastic scattering measurements. Resonance parameters for about 118 resonances formed by  $s$ -,  $p$ -, and  $d$ -wave neutrons have been determined. For each  $l$  value, individual strength functions for forming compound states for each allowable  $J$  have been examined for indications of doorway states. The presence of such a state at  $\sim 450$  keV in the  $J^\pi = 1^-$ ,  $s$ -wave channel has been confirmed, but the reported doorway state in the  $0^-$  channel at about 460–480 keV has been shown not to exist. However, a  $0^-$  resonance

having considerable strength was observed at 228.49 keV.

A doorway state has been observed in the  $J^\pi = 1^+$ ,  $p$ -wave channel. In another work,<sup>7</sup> we have shown this doorway state to be correlated with the  $M1$  ground-state photon channel. Our data also suggest the possible presence of a doorway state in the  $J^\pi = 2^+$  channel.

Although the number of  $d$ -wave resonances is small, the plots of  $\sum \Gamma_n^2$  vs  $E_n$  for each  $J$  value are suggestive of microstructure. In the  $J^\pi = 1^-$  channel there is an indication of a possible correlation of the ground-state radiation width with the  $l=2$  reduced neutron width in the vicinity of the 256-keV resonance.

### ACKNOWLEDGMENTS

We are deeply indebted to C. H. Johnson, R. B. Perez, G. de Saussure, D. K. Olsen, and G. F. Auchampaugh for making available the computer codes DCON, SIOB, and MULTI. Thanks are due G. R. Satchler for enlightening discussions pertaining to strength functions and doorway states. Mr. Rick Snodgrass was kind to write a program for calculating differential cross sections. We acknowledge the contributions of Jack Craven for computer programs and the operating crew at ORELA. This research was sponsored by the Division of Basic Energy Science, U. S. Department of Energy under contract No. W-7405-eng-26 with Union Carbide Corporation.

<sup>1</sup>B. Block and H. Feshbach, *Ann. Phys. (N.Y.)* **23**, 47 (1963).

<sup>2</sup>C. Shakin, *Ann. Phys. (N.Y.)* **22**, 373 (1963); A. K. Kerman, L. S. Rodberg, and J. E. Young, *Phys. Rev. Lett.* **11**, 422 (1963); H. Feshbach, A. K. Kerman, and R. H. Lemmer, *Ann. Phys. (N.Y.)* **41**, 230 (1967).

<sup>3</sup>A. M. Lane and D. Robson, *Phys. Rev.* **151**, 774 (1966); D. Robson and A. M. Lane, *ibid.* **161**, 982 (1967).

<sup>4</sup>J. A. Farrell, G. C. Kyker, Jr., E. G. Bilpuch, and H. W. Newson, *Phys. Lett.* **17**, 286 (1965); F. T. Seibel, E. G. Bilpuch, and H. W. Newson, *Ann. Phys. (N.Y.)* **69**, 451 (1972).

<sup>5</sup>W. P. Beres and M. Divadeenam, *Phys. Rev. Lett.* **25**, 596 (1970). See also M. Divadeenam, W. B. Beres, and H. W. Newson, *Ann. Phys. (N.Y.)* **80**, 231 (1973); M. Divadeenam and W. P. Beres, in *Statistical Properties of Nuclei*, edited by J. B. Garg (Plenum, New York, 1972), p.579.

<sup>6</sup>S. F. Mughabghab and D. I. Garber, Brookhaven National Laboratory Report BNL-325 (National Technical Information Service, Springfield, Virginia, 1973) (unpublished) 3rd ed. Vol. 1.

<sup>7</sup>D. J. Horen, J. A. Harvey, and N. W. Hill, *Phys. Lett.*

**67B**, 268 (1977); *Phys. Rev. Lett.* **38**, 1344 (1977).

<sup>8</sup>D. C. Larson, C. H. Johnson, J. A. Harvey, and N. W. Hill, Oak Ridge National Laboratory Report ORNL/TM-5612, 1976 (unpublished).

<sup>9</sup>C. H. Johnson, M. Patterson, E. Long, J. Munro and J. L. Fowler, private communication, 1977 (unpublished).

<sup>10</sup>G. de Saussure, D. K. Olsen, and R. B. Perez (private communication); *Nucl. Sci. Eng.* **61**, 496 (1976).

<sup>11</sup>G. F. Auchampaugh, Los Alamos Scientific Laboratory Report LA-5473-MS, 1974 (unpublished).

<sup>12</sup>A. M. Lane and R. G. Thomas, *Rev. Mod. Phys.* **30**, 257 (1958).

<sup>13</sup>J. M. Blatt and L. C. Biedenharn, *Rev. Mod. Phys.* **24**, 258 (1952).

<sup>14</sup>B. J. Allen, R. L. Macklin, R. R. Winters, and C. Y. Fu, *Phys. Rev. C* **8**, 1504 (1973).

<sup>15</sup>R. J. Holt, R. M. Laszewski, and H. E. Jackson, *Phys. Rev. C* **15**, 827 (1977).

<sup>16</sup>C. D. Bowman, R. J. Baglan, B. L. Berman, and T. W. Phillips, *Phys. Rev. Lett.* **25**, 1302 (1970).

<sup>17</sup>R. E. Toohy and H. E. Jackson, *Phys. Rev. C* **6**, 1440 (1972).

<sup>18</sup>L. R. Medsker and H. E. Jackson, Phys. Rev. C 9, 709 (1974); L. C. Haache and K. G. McNeill, Can. J. Phys. 53, 1422 (1975).

<sup>19</sup>W. W. True, C. W. Ma, and W. T. Pinkston, Phys. Rev. C 3, 2421 (1971).

<sup>20</sup>See for example, J. E. Lynn, *The Theory of Neutron*

*Resonance Reactions* (Clarendon, Oxford, 1968) p. 688.

<sup>21</sup>S. Raman, M. Mizumoto, and R. L. Macklin, Phys. Rev. Lett. 39, 598 (1977); and private communication (unpublished).